Clays and Clay Minerals, Vol. 40, No. 4, 436–445, 1992.

CRYSTALLOCHEMICAL STUDY OF A POPULATION OF PARTICLES IN SMECTITES FROM A LATERITIC WEATHERING PROFILE

S. PETIT,[1] T. PROT,[1] A. DECARREAU,[1]
C. MOSSER,[2] AND M. C. TOLEDO-GROKE[3]

[1] Laboratoire de Pétrologie de la Surface, URA CNRS 721, Université de Poitiers
40, av. du Recteur Pineau, 86022 Poitiers Cédex, France

[2] Centre de Geochimie de la Surface, LP CNRS 6251, 1 rue Blessig
67084 Strausbourg Cédex, France

[3] Instituto de Geosciencias, USP, CP 20899, 01498 São Paulo, Brazil

Abstract—In the copper deposit of Salobo 3A (Brazil), nontronite-like clay samples were found at the bottom of the weathering blanket. Samples were fractionated first by sedimentation and then by a HGMS method. From XRD data, it was found that the samples are essentially smectite with kaolinite in very small quantities. The average structural formula of the smectite, presented in the traditional manner, is:

$$(Si_{3.59}Al_{0.41})O_{10}(Fe_{1.53}Al_{0.39}Mg_{0.08}Ti_{0.01}Cu_{0.02})(OH)_2$$
$$(Ca_{0.12}Na_{0.09}K_{0.01}Cu_{0.02})$$

Chemical analyses show that the smectite samples contain a population of clay particles whose chemistry ranges between a nontronite end-member and an Al-Mg beidellite end-member.

Spectroscopic studies by FTIR, Mössbauer, and ESR show that the three major octahedral cations (Al, Fe, Mg) are present in each octahedral sheet of the smectite, forming a solid solution, and that the chemical trends of the smectite clay detected at a "macroscopic" scale (associated clay particles) can also be observed at the unit cell scale.

Key Words—Crystal-chemistry, ESR, FTIR, Layer structural composition, Mössbauer, Nontronite, Smectite, Solid-solution.

INTRODUCTION

A few recent papers have shown that clay samples of various natures and described as monomineralic (generally from XRD data) are, in fact, composed of populations of clay particles having more or less variable chemical compositions. These works concern smectites (e.g., Paquet *et al.*, 1982, 1983; Nadeau *et al.*, 1985) and more recently the Garfield nontronite (Kerm, 1988). The variability of the clay particles chemistry is often related to the geochemical environment of their formation (Nadeau and Bain, 1986; Duplay, 1984; Duplay *et al.*, 1986).

The elemental analysis of clay particles can be obtained either by physical fractionation or by direct analysis using a TEM microscope equipped with energy dispersive X-ray facilities. In both cases, the obtained chemical analyses are those of several associated layers. So two important questions remain:

(1) Are the observed chemical variations of clay particles due to chemical changes from one layer to another, or are they due to chemical variations within some or all the layers?
(2) When several octahedral cations occur simultaneously in the clay structure, are they randomly distributed or clustered?

Answers to these questions can be obtained, in favorable cases, by using spectroscopic methods sensitive to the local order-disorder phenomena.

In a previous paper, such an approach was applied to a Ni-rich smectite from a lateritic weathering profile and with a strong clustering of octahedral cations in the mixed trioctahedral and dioctahedral layers or domains (Decarreau *et al.*, 1987).

The samples studied here are iron-rich smectites (nontronites) occurring in lateritic profiles (Toledo-Groke, 1986; Toledo-Groke *et al.*, 1987, 1989a, b). Previously, smectites with similar chemical compositions were studied by Mössbauer spectroscopy (Goodman *et al.*, 1976; Cardile and Johnston, 1985; Cardile *et al.*, 1986), but without data concerning the geological origin of samples. The aim of this paper was to determine, from a crystallochemical point of view, the origin of the chemical heterogeneity of iron-rich smectites often found in lateritic weathering profiles.

MATERIALS AND METHODS

The copper stratiform deposit of Salobo 3A, Serra Dos Carajas, northern Brazil, consists of a metasedimentary sequence called the Salobo-Pojuca's formation. It is located about 520 km SSW of Belem (50°W 6°S) in the southeastern part of the Amazonian forest. Under humid tropical climatic conditions, the weathering product of this Proterozoic formation is an al-

Table 1. Size fractions (wt. %) obtained by centrifugation and sedimentation procedures from the two bulk A and B samples.

Samples	Particle size fractions		
	0–1 μm	1–2 μm	2–50 μm
A	34	1	65
B	25	1	74

teration blanket about 65 m thick. Toledo-Groke (1986) observed a green clayey product in centimeter fissures in parent rock at the base of the blanket. In strongly fractured rock, a mixture of this clayey product with ferruginous minerals was observed.

Two samples (A and B) representative of the green clay, previously characterized as a cupriferous nontronite (Toledo-Groke *et al.*, 1987), were extracted from a horizontal drift of Salobo 3A mine. The very green color of these two samples suggested a very low level of contamination by other iron phases.

Samples A and B were first gently ground in an agate mortar and separated into 3 size fractions (<1, 1–2 and >2 μm) by centrifugation and sedimentation procedures. The weight percent of the size fractions obtained in this way are reported in Table 1. In the present study, only the <1 μm clay size fractions were examined because a small amount of goethite and hematite was detected by XRD analyses in the coarsest fraction and because the 1–2 μm size fractions were not abundant.

High-gradient magnetic separation (HGMS) was used to separate clay particles with different iron contents (Righi and Jadault, 1988). Suspensions of clay-size particles (<1 μm) were passed, by means of a peristaltic pump, through a magnetic filter at increasing fields from 0.025 T to 1.0 T. At each magnetic field value, separated clays were collected and named, for example, *A MAG-0.025*. The clay fraction which was not retained by the filter, was then sorted using a higher magnetic field. For the last magnetic field value (1.0 T), 2 fractions were obtained, one magnetic (*MAG-1.0*) and one non-magnetic (*NO MAG-1.0*). Table 2 shows the weight percent of the magnetic clay fractions obtained by HGMS for the A and B samples.

To be sure that spectroscopic data were not distorted by free Fe, deferration was made by a photolytic method using ammonium oxalate and oxalic acid (Tamm's solution) under U.V. (De Endredy, 1963). This method was used instead of treatment with citrate bicarbonate dithionite (CBD) solutions, because CBD treatment may cause partial reduction of Fe^{3+} in clay structures (Ericsson *et al.*, 1984) or structural changes in smectites (Cardile *et al.*, 1987). After deferration, all samples were soft green, and X-ray diffraction (XRD) and infrared (IR) data of the clay fraction were identical before and after deferration indicating the good preservation of the clay structure.

Several saturations of clay samples were made: with Li for Hoffman and Klemen's test (Hoffman and Klemen, 1950; Greene-Kelly, 1953), with Cs to indicate the vacancy distribution by XRD, and with K to ensure a better dehydration of samples for IR studies and because this is commonly the reference state of clays for IR spectroscopy.

Chemical analyses of bulk samples were performed by atomic absorption spectroscopy (AAS) with a Perkin Elmer 2380 instrument. Chemical analyses and TEM observations of clay particles were made on a transmission electron microscope (TEM) Jeol 100 CX, at 100 kV accelerating voltage and equipped with an energy dispersive X-ray system (University of Orléans, France). The samples were dispersed on a nickel-coated microgrid. The diameter of the electron beam is approximately 500 Å.

Clay fractions were characterized by XRD using a Philips PW 1730 diffractometer with Fe-filtered CoKα radiation (40 kV and 40 mA). IR spectra were recorded in the 400–4000 cm^{-1} range on a Nicolet 510 FT-IR spectrometer. The disks were prepared by mixing 3 mg sample with 200 mg KBr.

^{57}Fe Mössbauer spectra were recorded over the range ±4.2 mm/s in 512 channels on an Elscint AME 30 spectrometer (Métallurgie Physique Laboratory, University of Poitiers, France). A ^{57}Co/Rh source of nominal activity 25 mCi was used. The spectrum was obtained at room temperature for the powder and the background count was of the order of 2×10^6. Signals were recorded on a multichannel analyzer and isomer shifts were calculated with respect to α Fe metal. The absorber sample contained less than 10 mg Fe/cm^2 to avoid linebroadening effects due to absorber thickness (Bancroft, 1973). Deconvolutions, based on least squares fitting procedures, assumed Lorentzian lineshapes. Each absorption doublet was characterized by the isomer shift, quadrupole splitting, peak intensity, and line width. All these parameters could be constrained. The χ^2 and misfit values were used to measure the "goodness" of the computer fit.

ESR measurements were performed at 298 K on an X-band BER-400 Brüker spectrometer, using 100 kHz modulation and 20 mW incident microwave power (Université Catholique de Louvain, Belgium).

Table 2. Clay fractions (wt. %) obtained by HGMS from the 0–1 μm clay-size fraction for both A and B samples.

	MAG 0.025	MAG 0.05	MAG 0.075	MAG 0.1	MAG 0.25	MAG 0.5	MAG 1.0	NO MAG 1.0
A	10.0	20.9	8.4	8.4	26.4	3.4	6.7	15.8
B	7.7	19.2	7.7	7.7	7.7	3.9	7.7	38.4

https://doi.org/10.1346/CCMN.1992.0400408 Published online by Cambridge University Press

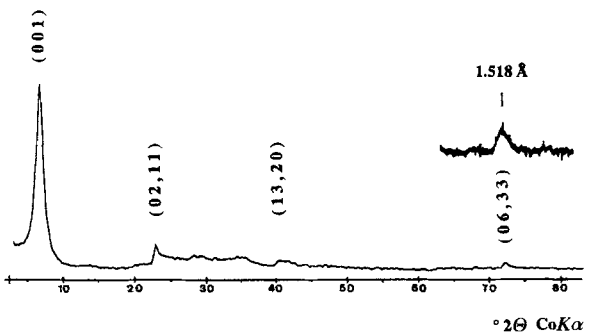

Figure 1. X-ray powder diffraction patterns of the smectitic clay sample *A MAG-0.05*.

RESULTS

X-ray diffraction data

Characterization. Powder patterns exhibit asymmetric (*hk*) bands characteristic of a turbostratic stacking of layers. They show diffraction intensity maxima corresponding to positions of the (02,11) and (13,20) bands of smectite and an intense (001) basal reflection (Figure 1). For all magnetic fractions, the smectitic clay sample seems to consist solely of a swelling dioctahedral smectite. For the non-magnetic fractions, very small quantities of kaolinite can also be observed. The (06,33) reflection shows a strong maximum at 1.518 Å, giving a *b*-parameter value of 9.12 Å. This value is usually observed for iron-rich dioctahedral smectites (e.g., Brigatti, 1983).

XRD patterns of air-dried oriented fractions (Figure 2), show an intense peak at 14.86 Å (001 reflection) and a weaker one at 7.51 Å. After saturation by ethylene glycol, this mineral expands, and a (001) peak at 17.10 Å and a (002) peak at 8.60 Å were visible indicating the swelling of all the layers and the lack of

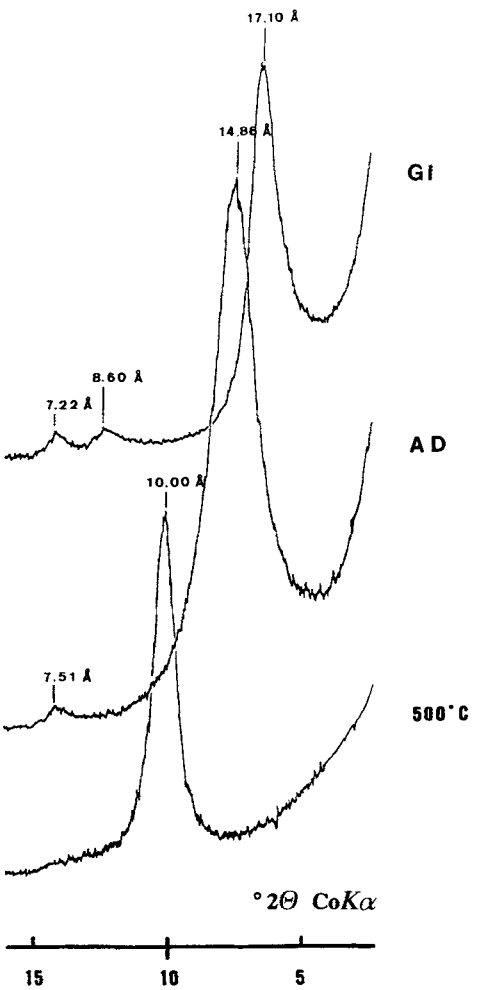

Figure 2. XRD patterns of oriented aggregates (*A MAG-0.05*). (AD: air dried; GI: glycolated; and after heating for 2 hr at 500°C).

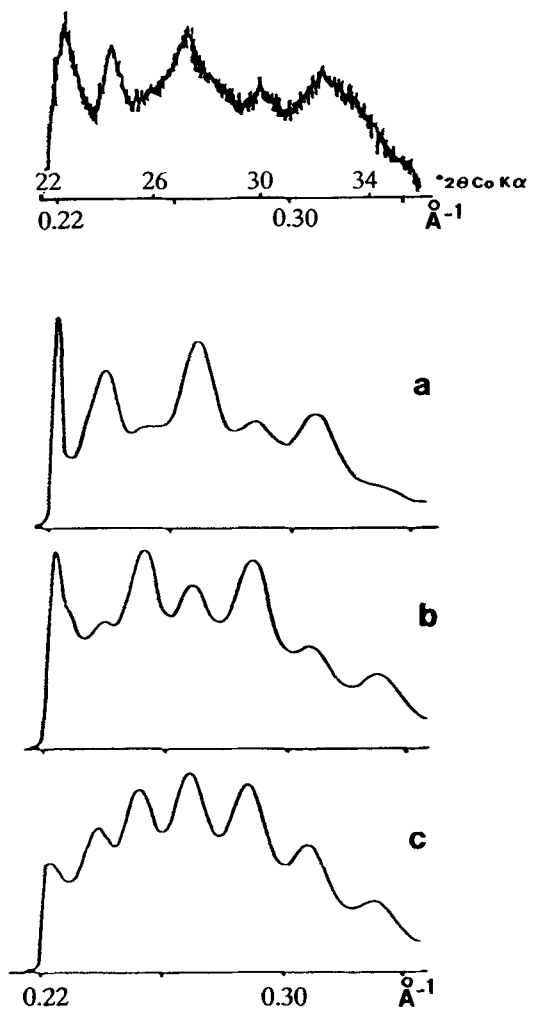

Figure 3. X-ray diffraction bands (02*l*,11*l*) after Cs-saturation of sample *A MAG-0.075* (top) and calculated models for the distribution of octahedral cations (from Besson *et al.*, 1983a). (a) Vacant *trans* octahedra; (b) vacant *cis* octahedra; (c) each octahedral site equally occupied.

https://doi.org/10.1346/CCMN.1992.0400408 Published online by Cambridge University Press

Table 3. Chemical analyses (wt. %) of smectitic clay calculated on the basis of the sum of oxides equal to 100. Samples from 1 to 7 are from the microprobe analysis of bulk smectitic clay by Toledo-Groke (1986). The others are different magnetic fractions of A and B.

Sample	SiO_2	Fe_2O_3	Na_2O	K_2O	Al_2O_3	MnO	MgO	CaO	TiO_2	CuO
1	55.24	27.54	0.03	0.03	12.72	0.03	0.81	1.33	0.01	2.25
2	58.35	24.27	0.13	0.03	13.18		0.85	1.54		1.66
3	57.22	25.46	0.05	0.02	13.41	0.02	0.84	1.75		1.19
4	58.33	24.73		0.01	12.77	0.06	0.70	1.86	0.01	1.53
5	57.24	23.34			15.16	0.19	1.01	1.26		1.79
6	55.23	26.98	0.03	0.07	13.46		0.89	1.13		2.19
7	54.58	27.85			12.82		0.77	0.99		2.99
A MAG 0.025	52.74	31.85	0.78	0.17	11.09	0.01	0.90	1.37	0.20	0.90
MAG 0.075	54.64	29.78	0.58	0.16	11.20	0.01	0.82	1.70	0.22	0.89
MAG 0.10	52.81	32.32	0.48	0.16	10.79	0.01	0.83	1.52	0.21	0.87
MAG 0.25	53.66	31.47	0.46	0.17	10.54	0.01	0.85	1.72	0.29	0.88
MAG 0.50	53.97	31.19	0.48	0.19	10.51	0.01	0.81	1.67	0.33	0.83
MAG 1.0	55.03	29.26	0.70	0.17	10.97	0.01	0.84	1.81	0.35	0.86
NO MAG 1.0	54.91	28.69	0.62	0.18	11.69	0.01	0.89	1.79	0.35	0.86
B MAG 0.025	51.63	29.4	0.84	0.16	13.61	0.04	0.96	0.02	0.12	1.22
MAG 0.05	54.56	27.92	0.59	0.10	12.98	0.03	0.93	1.57	0.10	1.21
MAG 0.075	55.21	27.07	0.52	0.11	12.96	0.03	0.89	1.97	0.09	1.15
MAG 0.10	55.04	27.44	0.56	0.13	12.39	0.03	0.86	2.33	0.07	1.15
MAG 0.25	55.35	26.71	0.62	0.13	12.57	0.03	0.87	2.56	0.11	1.06
MAG 0.50	53.11	27.17	0.40	0.17	13.06	0.04	1.54	3.20	0.13	1.13
NO MAG 1.0	55.58	25.95	0.56	0.10	13.62	0.03	0.86	2.02	0.09	1.19

mixed layer clay minerals. For some samples, a third broad peak with a very low intensity at 7.22 Å was attributed to kaolinite (Brindley and Brown, 1980). After heating the sample for 2 hr at 500°C, a single reflection remains at 10 Å.

Crystal size coherency is quite constant for all magnetically separated fractions. The measured values obtained by the Scherrer equation were 75–90 Å along (c*) and 205–215 Å in the (a-b) plane.

Location of the layer change. After Li-saturation, heating for 12 hr at 250°C (a platinum crucible was used to avoid the exchange of Li to Na, as observed with soda–lime glass by Byström-Brusewitz 1976), saturation with ethylene glycol was carried out. The samples showed an intense peak at 16.82 Å demonstrating an expandable clay mineral having a tetrahedral charge, i.e., a beidellite.

Position of the octahedral vacancy. Because poorly crystalline smectites show weak and diffuse *hkl* reflections, it is not possible to determine with accuracy, using normal diffraction methods, the atomic distribution within the octahedral sheet or the vacancy position (*cis* or *trans*). The use of Cs as the interlayer cation produces an increase of the *hkl* reflection intensities and the stacking order of the unit layers also increases (Besson *et al.*, 1983a).

Saturation with Cs was performed for the sample *A MAG-0.075*. The XRD pattern gave the 02(*l*) and 11(*l*) reflections (Figure 3) which are compared qualitatively with different patterns calculated by Besson *et al.* (1983a) for dioctahedral Cs-saturated smectites having *trans* vacant (all M_2 sites occupied), *cis* vacant (M_1 and 1/2 M_2 sites occupied), or M_1 and M_2 octahedral sites randomly occupied. The experimental pattern corresponds clearly to dioctahedral layers with a marked "*trans* vacant" character. According to Besson *et al.* (1983a), this approach is qualitative and a small quantity (less than 5%) of *trans* occupied sites cannot be completely excluded for the studied samples.

Chemical analyses

Chemical analyses of samples A and B measured by AAS are reported in Table 3. Structural water content (obtained by the weight loss after heating to 1000°C) could be measured for only one fraction (*B NO MAG-1-0*), due to the low quantity of clay; it was 22 wt. %.

Chemical analyses show only slight irregular variations in the total Fe_2O_3 content of the different fractions as the magnetic field increases whereas Al_2O_3 remains almost constant. No strictly ferric clay could be separated. These results show the partial failure of HGMS, in this case, to sort clay particles.

Though chemical data are almost homogeneous, it is notable that CuO contents measured by Toledo-Groke (1986) are slightly higher than for the different magnetic fractions of both A and B samples. This can be due to the different methods used (microprobe for Toledo-Groke samples and AAS for A and B samples) and the different scales of observation.

Al, Fe, and Mg analyses of the smectitic clay obtained by AAS are plotted within a triangular diagram of octahedral composition (Figure 4) (Weaver and Pollard, 1973). Chemical analyses of particles from the different magnetic fractions for both A and B samples, obtained by TEM are also plotted. Chemical data ap-

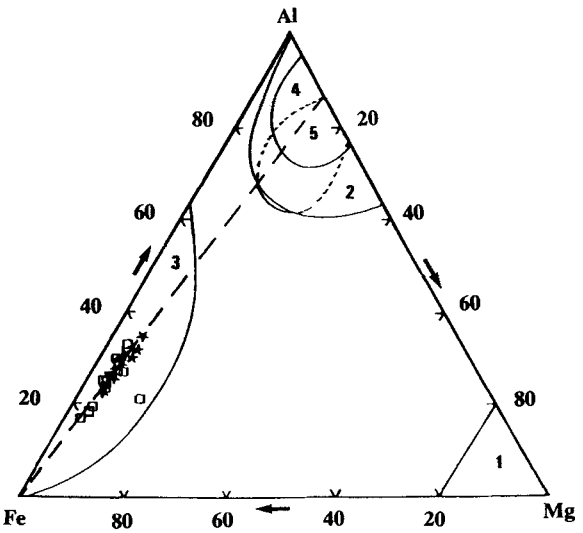

Figure 4. Al, Fe, and Mg variations in the smectitic clay (★: analyses obtained by AAS; □: TEM analyses of particle) plotted in the triangular diagram of Weaver and Pollard (1973). (1) Trioctahedral smectite; (2) montmorillonite; (3) nontronite; (4) illite; (5) illite/smectite mixed layer.

pear consistent from the macroscopic scale (microprobe analyses and analyses of physically separated fractions of sample) to the clay particle scale (TEM analyses). The plots are distributed in the nontronite domain, on a line joining the ferric end-member (pure nontronite) to an Al-Mg end-member (14% Mg). This line suggests the occurrence of a solid solution between a pure Fe nontronite and an Al + Mg beidellite.

The cation exchange capacities (CEC) determined by ammonium acetate method of Jackson (1958) at pH 7 on bulk samples A and B are of the order of 78 meq/100 g. The studied clay samples are low charge smectites. Exchangeable cations, including Cu, were determined by titration for 3 samples (*A MAG-0.025*; *A MAG-1.0*; *A NO MAG-1.0*). By comparison with total Cu content of these clays, almost half the Cu seemed to be in the octahedral sheet.

An average structural formula for the bulk sample can be calculated as:

$$(Si_{3.59}Al_{0.41})(Fe_{1.53}Al_{0.39}Mg_{0.08}Ti_{0.01}Cu_{0.02})O_{10}(OH)_2$$
$$(Ca_{0.12}Na_{0.09}K_{0.01}Cu_{0.02}).$$

Iron is expressed as Fe^{3+} according to Mössbauer spectroscopic data (see below). The theoretical CEC calculated from this structure, at 77 meq/100 g, is in agreement with experimental data. Taking into account uncertainties in chemical analyses, only two octahedral sites are occupied and this smectite is dioctahedral.

Transmission electron microscopy

The less than 1 μm fraction of the smectitic clay consists of abundant, elongated lath-shaped particles

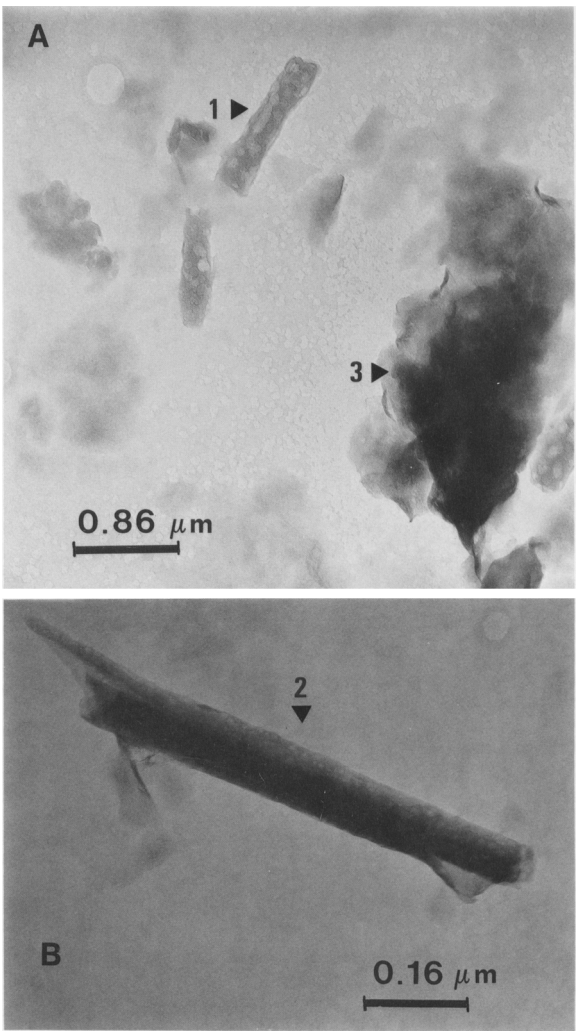

Figure 5. Transmission electron micrographs of the smectitic clay sample. A: (1) Elongated lath-shaped particle and (3) irregular folliated particle. B: (2) Elongated lath-shaped particle.

(1, Figure 5A and 2, Figure 5B) and irregular foliated particles (3, Figure 5A) having diffuse boundaries and irregular surface topography. These morphological features are often found in other nontronite-like clays (Güven, 1988). Isolated particles attain a length of about 1 μm and a width of 0.2–0.3 μm. Figure 5B shows an isolated rolled-up particle. Probably, this form results from dehydration conditions. It seems that these particles contain fewer layers than the others.

Infrared spectroscopy

IR spectra were recorded after K-saturation and dehydration of the smectitic clay sample. They are similar for each fraction and are almost similar to the IR spectrum of nontronite (Goodman *et al.*, 1976), but differ by having additional vibrations at 3698, 3620, and 913

https://doi.org/10.1346/CCMN.1992.0400408 Published online by Cambridge University Press

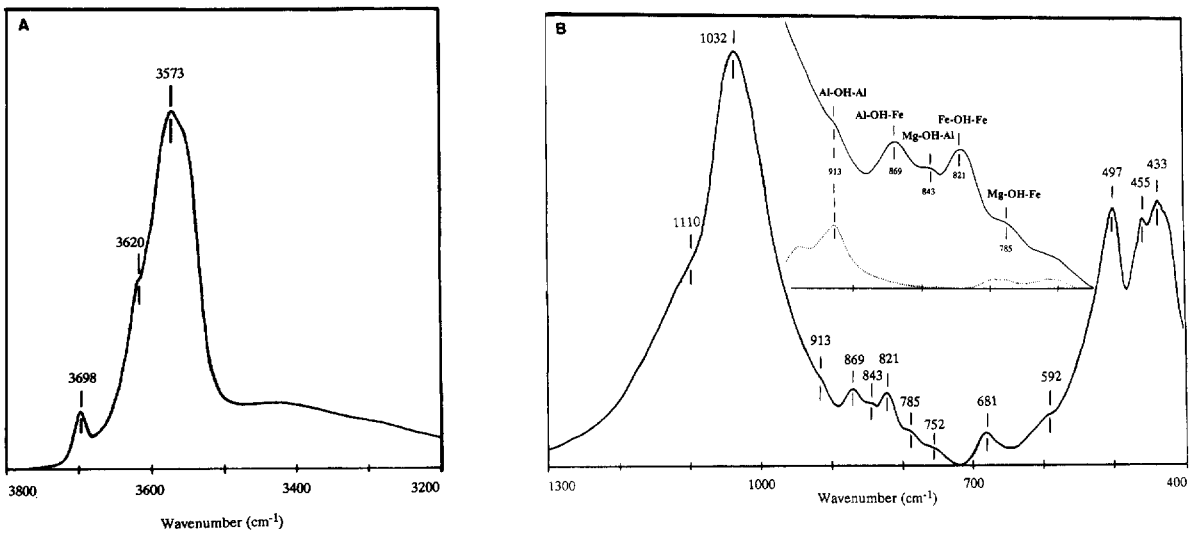

Figure 6. IR spectrum of the smectitic clay after K-saturation and dehydration at 200°C. A: OH stretching vibrations zone. B: The 1200–400 cm^{-1} region; dotted line in enlarged region estimates the kaolinite contribution.

cm^{-1}. These frequencies are attributed to Al_2OH group vibrations characteristic of kaolinite (Farmer and Russell, 1964). Kaolinite is detected in all fractions. As previously observed by Delvaux *et al.* (1989), IR spectroscopy gives a more sensitive indication of kaolinite than XRD. Kaolinite content detected by IR increases with the increasing magnetic field value of the fraction and, in accordance with XRD data, the non-magnetic fractions are the most kaolinite-rich.

OH stretching region (Figure 6A). The smectitic clay contains interlayer water which is outlined by the broad band centered at 3420 cm^{-1}. An intense OH stretching absorption band is noted at 3573 cm^{-1}, this occurring in the frequency range of $Fe_2^{3+}OH$ stretching vibrations in nontronite (Goodman *et al.*, 1976). The two bands at 3698 and 3620 cm^{-1} attributed to kaolinite "impurity" may hide other shoulders.

The 1300–400 cm^{-1} region (Figure 6B). An intense Si-O stretching absorption band is observed at 1032 cm^{-1} (Figure 6B). Following Goodman *et al.* (1976), this feature indicates that the smectite has no tetrahedral Fe^{3+} substitutions. Lattice vibration bands are noted at 681, 497, and 433–455 cm^{-1} as in typical nontronite IR spectra (Stubican and Roy, 1961; Goodman *et al.*, 1976).

Figure 6B presents details of the OH bending vibrations region. Samples show 3 absorption bands at 869, 843, and 821 cm^{-1}, and a shoulder at 785 cm^{-1}. The 869 cm^{-1} band is assigned to AlFeOH vibrations (Russell *et al.*, 1970; Farmer, 1974). Cracium (1984) observed for montmorillonites a relationship between octahedral Fe^{3+} content and the intensity and position of the absorption band due to AlOHFe vibrations. The wavenumber of AlOHFe vibrations band decreases with increasing octahedral Fe^{3+} content to almost 880 cm^{-1} or 870 cm^{-1}. The 869 cm^{-1} band confirms the high octahedral Fe^{3+} content of the samples.

The 821 cm^{-1} band is attributed to $Fe_2^{3+}OH$ vibrations, while the shoulder at 785 cm^{-1} may be attributed to $Fe^{3+}OHMg^{2+}$ vibrations (Farmer, 1974; Goodman *et al.*, 1976).

Assignment of the 843 cm^{-1} band is not well established. Goodman *et al.* (1976) observed a similar band for nontronites showing a very high octahedral iron content and high tetrahedral charge, but it does not occur for the Washington nontronite sample which has nearly the same chemical composition (low tetrahedral charge) as our samples. In this case, Goodman *et al.* (1976) attributed the band to AlOHFe vibrations, after rejecting, on the basis of Mössbauer spectroscopic results, the possibility of assigning this band and the 820 cm^{-1} one to vibrations of OH groups in *trans* and *cis* octahedral configurations. Alternatively, Russell *et al.* (1970) and Cracium (1984) characterized an $Al^{3+}OHMg^{2+}$ vibration band at about 839–848 cm^{-1} in montmorillonite. Taking into account all the crystallographic and chemical data, it seems that this last assignment should be retained here.

Because all the cations pairs, evidenced via hydroxyl bonds by IR, are always present in the clay-size fractions or magnetic clay fractions, no chemical segregation of cations in octahedral sheets of the different clay populations can be implied. Furthermore, no specific features corresponding to Al or Mg clusters in the octahedral sheet of the smectite are observed. After simulation of the kaolinite contribution estimated from OH stretching vibrations region data, it is clear that the shoulder centered at almost 913 cm^{-1} which corresponds to the location of Al_2OH group bending vi-

https://doi.org/10.1346/CCMN.1992.0400408 Published online by Cambridge University Press

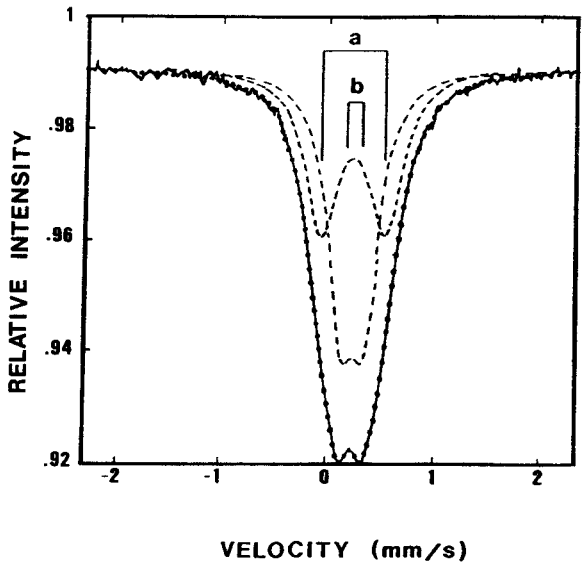

Figure 7. Mössbauer spectrum at room temperature of the smectitic clay sample, *A MAG-0.025*. Experimental data (full line) and fit (dotted line) using two doublets.

brations must be completely attributed to a very small amount of kaolinite (Figure 6B).

Mössbauer spectroscopy

Many papers have been published concerning the interpretation of Mössbauer spectra of nontronite, with more or less conflicting results. It is now well established that the predominant Fe^{3+} resonance is computer-fitted with two doublets defining Fe in non-equivalent M_2 [*cis*-$FeO_4(OH)_2$] octahedral sites. In most of the cases, improvement in the fit can be made by a Fe^{3+} tetrahedral contribution (Cardile and Johnston, 1985). The $^{IV}Fe^{3+}$ Mössbauer resonance lines can also be more easily evidenced when smectite samples are Ca-exchanged and dehydrated (Luca and Cardile, 1989; Luca, 1991).

Figure 7 shows the Mössbauer spectrum of the *A MAG-0.025* sample, which was previously deferrated. The experimental spectrum consists of one broad and almost symmetrical doublet with an isomer shift near 0.35 mm/s (*vs* Fe metal). These features are typical of octahedrally coordinated Fe^{3+}, excluding the occurrence of octahedral Fe^{2+} (Coey, 1980; Heller-Kallai and Rozenson, 1981). Several fits of the experimental spectrum were tested. The best one was obtained with only two doublets (Table 4). Values obtained for isomer shift and quadrupole splitting are similar to those previously obtained for octahedrally coordinated Fe^{3+} in nontronite (Goodman *et al.*, 1976; Besson *et al.*, 1983b; Bonnin *et al.*, 1985; Cardile and Johnston, 1985; Johnston and Cardile, 1985; Daynyak and Drits, 1987). Addition of a tetrahedral Fe^{3+} doublet does not improve the goodness of the fit. This result is consistent with IR data. All these data suggest that the studied sample contains no, or very small amounts of $^{IV}Fe^{3+}$. However, tetrahedral Fe is difficult to detect as is shown by the conflicting results obtained recently with the Garfield nontronite (Cardile, 1988; Sherman and Vergo, 1988; Luca, 1991).

Table 4. Values of the Mössbauer parameters for the smectitic clay sample.

	Isomer shift (mm/s)	Quadrupole splitting (mm/s)	Peak width (mm/s)	Area (%)
Doublet a	0.35	0.60	0.38	46
Doublet b	0.36	0.22	0.32	54

From Goodman (1978), Besson *et al.* (1983b), and Daynyak and Drits (1987), the outer doublet may be attributed to octahedral Fe^{3+} cations seeing the 3Si + Al combination for tetrahedral occupation. In this case, the intensity of the outer doublet is greater than that calculated on the basis of a random distribution of Fe^{3+} cations in the M_2 octahedral site, suggesting that Fe^{3+} cations are preferably connected with substituted tetrahedra. If we assumed that the recoilless fraction is the same for the different sites, the measured quadrupole splitting for the outer doublet is lower than predicted by Daynyak and Drits (1987) for such a neighborhood. This fact can be attributed to variable neighboring cations within the octahedral sheet, this one being $3R^{3+}$ or $2R^{3+}$-R^{2+} or R^{3+}-$2R^{2+}$, essentially. But no calculated quadrupole splitting values for the last combinations are available.

Electron spin resonance spectroscopy

Figure 8 shows the ESR spectrum at room temperature of the *A MAG-0.025* sample of smectitic clay. A broad resonance near g = 2 due to exchange coupling of two Fe^{3+} ions in adjacent sites (Meads and Malden, 1975) is observed. This broad band occurs generally for Fe-rich 2:1 clay minerals (Olivier *et al.*, 1975; Goodman *et al.*, 1988; Delvaux *et al.*, 1989) but also for Fe oxides (or oxy-hydroxides). The g = 2 signal cannot be attributed to a free iron oxide because these clay samples were previously completely deferrated and no oxide phase was seen by Mössbauer spectroscopy. Consequently, the g = 2 broad resonance indicates that Fe^{3+} cations are in neighbouring octahedral structural sites in the smectite.

For ferric smectites, Bonnin (1981) showed that ESR spectra of the Garfield nontronite can be fitted with only one Lorentzian line and Figure 8 shows the same possible decomposition of the ESR spectrum. So from ESR data, Fe^{3+} ions are located in nontronite-like layers or in nontronite domains in the octahedral sheet of clay particles. The small difference between the experimental spectrum and the fitted Lorentzian line may be attributed to Cu, but no clear feature is attributable to the Cu occurrence in the smectite.

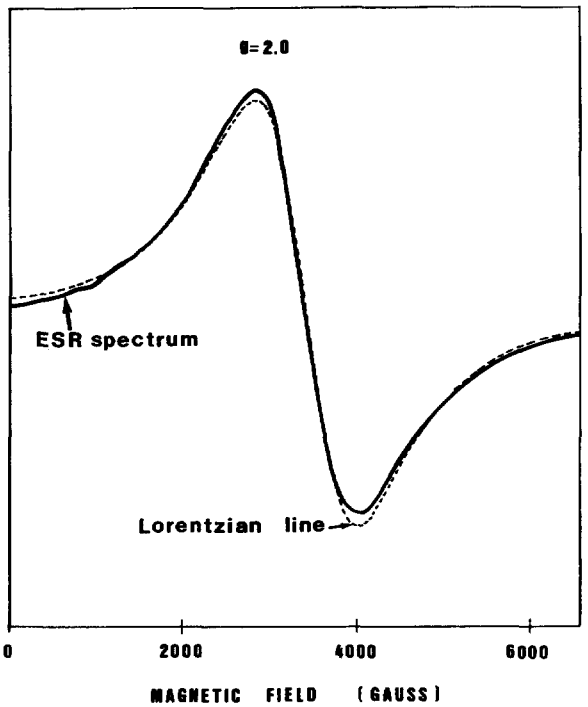

Figure 8. Decomposition with one Lorentzian line of the ESR spectrum of the smectitic clay.

DISCUSSION

From XRD data, the studied smectites are clearly dioctahedral. The layer charge is only tetrahedral and these smectites belong to the beidellite-nontronite group. After Cs saturation of the interlayer, it is possible to establish from XRD data that the *trans*-octahedral sites are unoccupied (within the uncertainty range of the measurements). A similar feature has been previously observed for nontronite samples (Besson *et al.*, 1983b), celadonite (Drits *et al.*, 1984), and ferripyrophyllite samples (Coey *et al.*, 1984). Most iron-rich dioctahedral 2:1 clays have their *trans*-octahedral sites vacant or only occupied at low levels.

TEM observations show clay particles which are essentially laths and secondary irregularly shaped particles. Qualitative chemical analyses carried out on isolated clay particles remain always the same, and the Al/Fe ratio measured on isolated clay particles are similar to those obtained on bulk samples. Clay particles containing only one octahedral cation, or possibly two, have not been observed. The HGMS method results do not show the occurrence of highly concentrated iron particles. The clay samples cannot be described as a mechanical mixture of smectites having a particular chemistry such as a dioctahedral one containing Fe and Al and a trioctahedral one containing Mg and Cu. Notably, no phase with a high Cu content such as chrysocolla was detected. The most important result obtained by chemical analyses is the alignment of individual analyses (Figure 4), suggesting that the clay samples are composed of particle populations corresponding to a mixing of two compositions, one only ferric, the other both aluminous and magnesian.

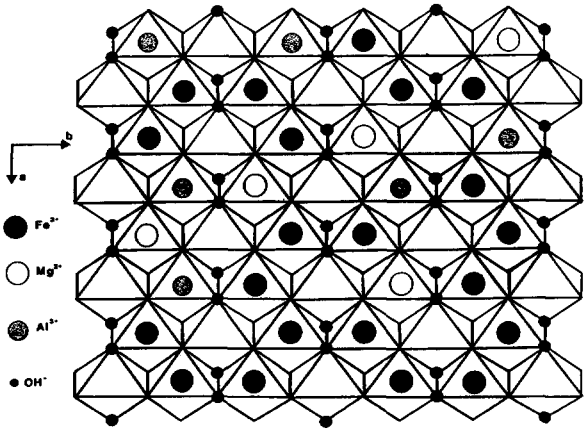

Figure 9. Projection in the a, b plane of the octahedral sheet of the smectitic clay.

From the above chemical results two different associations of octahedral cations are possible: (1) Al-Fe-Mg-Cu are mixed within each sheet of clay particles, and the nature of the solid solution is unknown (random distribution of cations or clustering); (2) some cations are segregated in some layers which are mixed to form a clay particle.

IR results clearly show that vibrational frequencies of OH corresponding to Al-Fe, Fe-Mg, and Al-Mg pairs are present. So, all the three major octahedral cations Al, Fe, and Mg are distributed in all the layers of the smectite samples.

Several independent spectroscopic results show that Fe atoms are concentrated within the octahedral sheets: (1) strong OH stretching and bending bands at 3573 and 818 cm^{-1}, respectively; (2) ESR signal with a Lorentzian line shape at $g = 2$. On the contrary, no specific features corresponding to Al or Mg clusters are observed, especially from IR results.

A schematic distribution of cations in the octahedral sheet of the smectites can be then drawn (Figure 9). The three major cations are located in M_2 sites of contiguous cells, but their distribution is not completely random. The chemical map of the octahedral sheet can be described as an iron matrix with dispersed Al-Mg zones. No particular location of these two last cations has been found. Two remarks can be made: (1) Because Fe cations in M_2 sites are 72% of the total octahedral population, even a random distribution of these cations in these sites is bound to give Fe clusters in spectroscopic analyses; (2) the two chemical poles found from Figure 4 exist at the scale of the smectite cells associated in clay layers. The chemical variations observed within the population of smectite particles must be explained by the relative importance of the two poles (Fe^{3+} on

https://doi.org/10.1346/CCMN.1992.0400408 Published online by Cambridge University Press

one hand, Al-Mg on the other) within each octahedral sheet. Surprisingly, the chemical poles are Al-Mg and Fe and not Al-Fe and Mg. Güven (1988) also observed that in dioctahedral smectites, coupled octahedral substitutions such as AlMg for Fe^{3+} (or $MgFe^{3+}$ for Al) seem to be favored over single substitutions such as Al for Fe^{3+}. This can be connected with the change in plane space group symmetry of smectite layers with their chemistry. As previously stated, in Fe-rich smectites, *trans*-octahedral positions are vacant. Al-Mg beidellites have either all the *trans*-octahedral sites occupied or the *trans* and *cis* sites randomly occupied (Besson *et al.,* 1983a; Tsipursky and Drits, 1984). So the more stable crystallographic structures of smectites are not the same when their chemistry varies, and the segregation of Fe, on one hand, and Al plus Mg, on the other hand, can be taken as a consequence of this rule. For these samples the *trans*-octahedral sites are mostly unoccupied, but a small number of *trans*-octahedral sites may contain Al or Mg atoms.

CONCLUDING REMARKS

The studied Fe-rich smectites formed in the lower part of lateritic weathering profiles exhibit limited chemical heterogeneity. This heterogeneity, which is easily observed at the microprobe scale (few micrometers), does not appear as a random distribution around a mean value, but as a mixing of two end-members: a nontronitic one and a beidellitic one. This chemical trend also is evident in clay-sized particles (less than 0.1 μm in diameter, and few stacked layers), and is due to the relative ratio of Fe, Al, and Mg in associated unit cells in individual clay layers. Each clay layer can be considered as a sample of a true solid-solution between the nontronite end-member and the beidellite end-member. The macroscopic chemical heterogeneity of the sample can be explained by a mixing of clay layers which exhibit a continuous chemical change along a solid-solution chemical line. These results contrast with those obtained for other lateritic Ni-Fe-Mg smectites (Decarreau *et al.,* 1987) which exhibit strong chemical segregations within clay particles.

As previously described by Garrels (1984) for illite/smectite stability diagrams, the knowledge of the origin of chemical changes in clay mineral compositions influences the thermodynamic approach to clay genesis. For a clay sample showing a chemical heterogeneity, as described above, the chemical activity diagrams are quite different depending on whether the clay is regarded as a solid-solution or as a mixture of two (or more) phases. The above results show that some clay minerals can be considered as true solid-solutions, but this may not always be the case.

ACKNOWLEDGMENTS

The authors are indebted to Dr. C. M. Cardile and Dr. J. M. Coey for their helpful reviews.

REFERENCES

Bancroft, G. M. (1973) *Mössbauer spectroscopy. An Introduction for Inorganic Chemists and Geochemists:* McGraw-Hill, London, 252 pp.

Besson, G., Glaeser, R., and Tchoubar, C. (1983a) Le césium, révélateur de structure des smectites: *Clay Miner.* **18,** 11–19.

Besson, G., Bookin, A. S., Daynyak, L. G., Rautureau, M., Tsipursky, S. I., Tchoubar, C., and Drits, V. A. (1983b) Use of diffraction and Mössbauer methods for the structural and crystallochemical characterization of nontronites: *J. Appl. Crytallog.* **16,** 374–383.

Bonnin, D. (1981) Propriétés magnétiques liées aux désordres bidimensionnels dans un silicate lamellaire ferrique: la nontronite. *Etude par spectrométrie Mössbauer, Résonances Magnétiques, Magnétisme ex EXAFS:* Thèse Sci., Univ. Paris VI, Paris, 82 pp.

Bonnin, D., Calas, G., Suquet, H., and Pezerat, H. (1985) Intracrystalline distribution of Fe^{3+} in Garfield nontronite: A spectroscopic study: *Phys. Chem. Minerals* **12,** 55–64.

Brigatti, M. F. (1983) Relationships between composition and structure in Fe-rich smectites: *Clay Miner.* **18,** 177–186.

Brindley, G. W. and Brown, G. (1980) *Crystal Structure of Clay Minerals and Their X-Ray Identification:* Mineralogical Society, London, 495 pp.

Byström-Brusewitz, A. M. (1976) Studies on the Li test to distinguish between beidellite and montmorillonite: in *Proc. Int. Clay Conf., Mexico City,* S. W. Bailey, ed., Applied Publishing, Wilmette, Illinois, U.S.A., 419–428.

Cardile, C. M. (1988) Tetrahedral Fe in smectites: A critical comment: *Clays & Clay Minerals* **37,** 185–188.

Cardile, C. M. and Johnston, J. H. (1985) Structural studies of nontronites with different iron contents by ^{57}Fe Mössbauer spectroscopy: *Clays & Clay Minerals* **33,** 295–300.

Cardile, C. M., Johnston, J. H., and Dickson, D. P. E. (1986) Magnetic ordering at 4.2 and 1.3 K in nontronites of different iron contents: A ^{57}Fe Mössbauer spectroscopic study: *Clays & Clay Minerals* **34,** 233–238.

Cardile, C. M., Childs, C. W., and Whitton, J. S. (1987) The effect of citrate/bicarbonate/dithionite treatment on standard and soil smectites as evidenced by ^{57}Fe Mössbauer spectroscopy: *Aust. J. Soil. Res.* **25,** 145–154.

Coey, J. M. D. (1980) Clay minerals and their transformations studied with nuclear techniques: The contribution of Mössbauer spectroscopy: *Atomic Energy Review* **18,** 73–124.

Coey, J. M. D., Chukhrov, F. V., and Zvyagin, B. B. (1984) Cation distribution, Mössbauer spectra and magnetic properties of ferripyrophyllite: *Clays & Clay Minerals* **32,** 198–204.

Cracium, C. (1984) Influence of the Fe^{3+} for Al^{3+} octahedral substitutions on the IR spectra of montmorillonite minerals: *Spectroscopy Letters* **17(10),** 579–590.

Daynyak, L. G. and Drits, V. A. (1987) Interpretation of Mössbauer spectra of nontronite, celadonite and glauconite: *Clays & Clay Minerals* **35,** 363–373.

Decarreau, A., Colin, F., Herbillon, A., Manceau, A., Nahon, D., Paquet, H., Trauth-Badaud, D., and Trescases, J. J. (1987) Domain segregation in Ni-Fe-Mg-smectites: *Clays & Clay Minerals* **35,** 1–10.

De Endredy, A. S. (1963) Estimation of free iron oxides in soils and clays by a photolytic method: *Clay Miner.* **29,** 209–217.

Delvaux, B., Mestdagh, M. M., Vielvoye, L., and Herbillon, A. J. (1989) XRD, IR and ESR study of experimental alteration of Al-nontronite into mixed layer kaolinite/smectite: *Clay Miner.* **24,** 617–630.

Drits, V. A., Plancon, A., Sakharov, B. A., Besson, G., Tsi-

pursky, S. I., and Tchoubar, C. (1984) Diffraction effect calculated for structural models of K saturated montmorillonite containing different types of defects: *Clay Miner.* **19,** 541–561.

Duplay, J. (1984) Analyses chimiques ponctuelles de particules d'argiles. Relation entre variations de composition dans une population de particules et température de formation: *Sci. Geol. Bull.* **37, 4,** 307–317.

Duplay, J., Desprairies, A., Paquet, H., and Millot, G. (1986) Celadonites et glauconites: double population de particules dans la celadonite de Chypre. Essai sur les températures de formation: *C.R. Acad. Sci. Paris* **302,** 181–186.

Ericsson, T., Linares, J., and Lotse, E. (1984) A Mössbauer study of the effect of dithionite/citrate/bicarbonate treatment on a vermiculite, a smectite and a soil: *Clay Miner.* **19,** 85–91.

Farmer, V. C. (1974) The layer silicates: in *The Infrared Spectra of Minerals,* V. C. Farmer, ed., Mineralogical Society, London, pp. 331–365.

Farmer, V. C. and Russell, J. D. (1964) The infrared spectra of layer silicates: *Spectrochim. Acta* **20,** 1149–1173.

Garrels, R. M. (1984) Montmorillonite/illite stability diagrams: *Clays & Clay Minerals* **32,** 161–166.

Goodman, B. A. (1978) The Mössbauer spectra of nontronites: Consideration of an alternative assignment: *Clays & Clay Minerals* **26,** 176–177.

Goodman, B. A., Nadeau, P. H., and Chadwick, J. (1988) Evidence for the multiphase nature of bentonites from Mössbauer and EPR spectroscopy: *Clay Miner.* **23,** 147–159.

Goodman, B. A., Russel, J. D., Fraser, A. R., and Woodhams, F. W. D. (1976) A Mössbauer and IR spectroscopic study of the structure of nontronite: *Clays & Clay Minerals* **24,** 53–59.

Greene-Kelly, R. (1953) The identification of montmorillonoids in clay: *J. Soil Sci.* **4,** 233–247.

Güven, N. (1988) Smectites: in *Hydrous Phillosilicates,* S. W. Bailey, ed., *Reviews in Mineralogy,* **19,** Mineral. Soc. Amer., Washington, D.C., 497–559.

Heller-Kallai, L. and Rozenson, I. (1981) The use of Mössbauer spectroscopy of iron in clay mineralogy: *Phys. Chem. Minerals* **7,** 223–238.

Hofmann, U. and Klemen, R. (1950) Verlust des Austauschfahigkeit von Lithiumionen an Bentonit durch Erhitzung: *Z. Anorg. Allg. Chem.* **262,** 95–99.

Jackson, M. L. (1958) *Soil Chemical Analysis:* 3rd ed: Prentice Hall, Englewood Cliffs, New Jersey, 498 p.

Johnston, J. H. and Cardile, C. M. (1985) Iron sites in nontronite and the effect of interlayer cations from Mössbauer spectra: *Clays & Clay Minerals* **33,** 21–30.

Kerm, A. G. (1988) Etude et caractérisation des premiers stades d'hydratation d'une nontronite: Thesis, University Orléans, 65 pp.

Luca, V. (1991) Detection of tetrahedral Fe^{3+} sites in nontronite and vermiculite by Mössbauer spectroscopy: *Clay & Clay Minerals* **39,** 467–477.

Luca, V. and Cardile, C. M. (1989) Improved detection of tetrahedral Fe^{3+} in nontronite SWa-1 through Mössbauer spectroscopy: *Clay Miner.* **24,** 115–119.

Meads, E. and Malden, P. J. (1975) Elecctron spin resonance in natural kaolinites containing Fe^{3+} and other transition metal ions: *Clay Miner.* **10,** 313–345.

Nadeau, P. H. and Bain, D. C. (1986) Composition of some smectites and diagenetic clays and implications for their origin: *Clays & Clay Minerals* **34,** 455–464.

Nadeau, P. H., Farmer, V. C., Mac Hardy,W. J., and Bain, D. C. (1985) Compositional variations of the Unterrupstroth beidellite: *Amer. Miner.* **70,** 1004–1010.

Olivier, D., Vedrine, J. C., and Pezerat, H. (1975) Application de la résonance paramagnétique électronique à la localisation du Fe^{3+} dans les smectites: *Bull. Groupe franç. Argiles* **XXVII,** 159–165.

Paquet, H., Duplay, J., and Nahon, D. (1982) Variations in the composition of phyllosilicates monoparticles in a weathering profile of ultrabasic rocks: in *Proc. 7th Inter. Clay Conf., AIPEA, Bologna-Pavia,* H. van Olphen and F. Veniale, eds., Der in Sedim., Elsevier **35,** 595–603.

Paquet, H., Duplay, J., Nahon, D., Tardy, Y., and Millot, G. (1983) Analyses chimiques de particules isolées dans les populations de minéraux argileux. Passage des smectites magnésiennes trioctaédriques aux smectites ferrifères dioctaédriques au cours de l'altération des roches ultra-basiques: *C.R. Acad. Sci. Paris* **296, D,** 699–704.

Righi, D. and Jadault, P. (1988) Improving soil clay minerals studies by high-gradient magnetic separation: *Clay Miner.* **23,** 225–232.

Russell, J. D., Farmer, V.C., and Velde, B. (1970) Replacement of OH by OD in layer silicates and identification of the vibrations of these groups in infra-red spectra: *Mineral Mag.* **37,** 869–879.

Sherman, D. and Vergo, N. (1988) Optical (diffuse reflectance) and Mössbauer spectroscopic study of nontronite and related Fe-bearing smectites: *Amer. Miner.* **73,** 1346–1354.

Stubican, V. and Roy, R. (1961) Isomorphous substitution and infrared spectra of the layer lattice silicates: *Amer. Miner.* **46,** 32–51.

Toledo-Groke, M. C. (1986) Intemperismo das rochas mineralizadas em cobre do Salobo 3A, Serra dos Carajas. Mecanismos de alteracao dos minerais primarios e localizaçao do cobre nos productos secundarios: Tese Dout., Instituto de Geociencias, Sao Paulo, Brazil, 173 pp.

Toledo-Groke, M. C., Melfi, A. J., and Parisot, J. C. (1987) Comportamento do cobre o intemperismo das rochas xistosas cupriferas do Salobo 3A, Serra dos Carajas: *Geochim. Brasil.,* 187–200.

Toledo-Groke, M. C., Boulangé, B., Parisot, J. C., and Melfi, A. J. (1989) Altération des biotites dans les roches cuprifères de Salobo 3A, Serra dos Carajas (Brésil). I; Formation des phyllosilicates secondaires: *Geodynamique* **4,** 135–150.

Toledo-Groke, M. C., Parisot, J. C., Melfi, A. J., and Boulangé, B. (1989) Altération des biotites dans les roches cuprifères de Salobo 3A, Serra dos Carajas (Brésil). II; Association du cuivre aux phyllosilicates secondaires: *Geodynamique* **4,** 151–160.

Tsipursky, S. I. and Drits, V. A. (1984) The distribution of octahedral cations in the 2:1 layers of dioctahedral smectites studied by oblique texture electron diffraction: *Clay Miner.* **19,** 177–193.

Weaver, C.E. and Pollard, L. D. (1973) *The Chemistry of Clay Minerals:* Elsevier, Amsterdam, 213 pp.

(Received 27 February 1992; accepted 22 July 1992; Ms. 2081)